

Azeotropic distillation with an internal decanter

Amy R. Ciric ^a, Hassan S. Mumtaz ^b, Grafton Corbett ^b, Matthew Reagan ^b,
Warren D. Seider ^{b,*}, Leonard A. Fabiano ^{c,1}, David M. Kolesar ^{c,2},
Soemantri Widagdo ^d

^a Department of Chemical Engineering, University of Cincinnati, Cincinnati, OH 45202-0171, USA

^b Department of Chemical Engineering, University of Pennsylvania, Towne Building D3, 220 S. 33rd Street, Philadelphia, PA 19104-6393, USA

^c Wayne, PA, USA

^d 3M, St Paul, MN 55144, USA

Received 14 June 1999; received in revised form 5 June 2000; accepted 7 June 2000

Abstract

A distillation column with an internal decanter is used to separate a mixture containing five some oxygenated and hydrocarbons and having at least three carbon atoms, and water. One of the species is partially miscible with water, as well as another organic species. Both binary pairs exhibit azeotropes above the minimum bubble-point temperature. The column is very sensitive to small disturbances which can lead to flooding, poor product quality, and migration of an embedded two-liquid phase region within the column. These disturbances can cause the column to move from one steady state to another for the same specifications. Multiple operating regimes are exhibited, with unusual transitions between them. Two regions involving multiple steady states are observed, one of which involves the partial-miscibility of two organic phases. The dynamics of moving interfaces between trays having one- and two-liquid phases, as well as controllers to insure that unwanted transitions do not occur, are examined. © 2000 Elsevier Science Ltd. All rights reserved.

Keywords: Azeotropic distillation; Internal decanter; Oxygenated hydrocarbons

1. Introduction

The sensitivity of azeotropic distillation columns with internal decanters to small disturbances can lead to flooding and the deterioration of distillate and sidedraw purities, from which it is difficult to return to normal operation. Thus far, this sensitivity and the disturbances that trigger shifts in the operating regimes have not been well understood. Furthermore, while there is an extensive literature on heterogeneous azeotropic distillation, that is, azeotropic distillation towers with two liquid phases on at least one of the trays or decanter, to our knowledge, azeotropic distillation columns with

internal decanters have not been studied in the literature (Widagdo & Seider, 1996).

This paper examines the behavior of columns with internal decanters, their operating regimes, and the existence of multiple steady states. In normal operation, these columns have a sidedraw composed of a single liquid phase, usually an aqueous phase, and two liquid phases on trays near the decanter tray. When operation in an anomalous regime occurs, there is only one liquid phase on the decanter tray and no sidedraw, two liquid phases appear on trays throughout the stripping section, the bottoms product contains two liquid phases, and the internal vapor flow rates are increased. Furthermore, small disturbances, such as an increase in the feed rate of the light species, can move these columns from normal to anomalous operation. It will be shown that the vapor flow is increased, which results in flooding when insufficient capacity is provided. For these reasons, it is an objective of this paper to show the sensitive responses to small disturbances, to show how

* Corresponding author. Tel.: +1-215-8988351; fax: +1-215-5732093.

E-mail address: seider@seas.upenn.edu (W.D. Seider).

¹ Present address: CDI Corporation, Philadelphia, PA 19103-2768, USA.

² Present address: Rohm & Haas Corporation, Bristol, PA 19007, USA.

multiple steady states arise, and to explore the dynamic responses of columns equipped with PID controllers.

This paper also examines a related behavior that occurs as the bottoms flow rate is reduced, resulting in an increased recirculation rate. Over a narrow range of the bottoms flow rate, two steady-state solutions are computed, one which involves only one liquid phase on the decanter tray and no sidedraw, and the other in which two partially-miscible organic phases form on the decanter tray, providing an organic sidedraw.

2. A typical ternary system

Columns with internal decanters are used commonly to remove one species, typically water, in a sidedraw that concentrates in one of two partially miscible phases. When designing and analyzing these columns, it is usually beneficial to focus attention on three principal species, one of which concentrates in the sidedraw, with the others concentrating in the distillate and bottoms product. Typical ternary systems have the residue-curve maps shown in Fig. 1. (Note that all possible residue-curve maps associated with internal decanters are not shown). Species A, the lowest boiler, is recovered in the distillate. It may form maximum-boiling azeotropes with water and species C, and, when two liquid phases are present, it often strongly prefers the liquid phase rich in species C. Water may be either the heavy or the intermediate boiler. It forms a heterogeneous minimum-boiling azeotrope with species C. While water is concentrated in a side stream from an internal decanter tray, species C is an intermediate or heavy boiler recovered in the bottoms stream. Often, species A is a light organic chemical and species C is a heavy organic chemical.

2.1. Phase equilibria and residue curves

In this section, physical and thermodynamic properties are presented for a specific, proprietary A–water–C system. This system is the subject of a theoretical and

experimental study of a distillation tower introduced in the next section. Note that care was taken to obtain interaction coefficients for the NRTL equation that represent both experimental VLE and LLE data with acceptable accuracy.

To understand the interactions within the system, the binary pairs are considered first. Fig. 2 shows the bubble- and dew-point curves for the three binary pairs at near-atmospheric pressure, computed using ASPEN PLUS™. The water–C system exhibits a minimum-boiling azeotrope at 75 mol% water and 97.2°C and a large miscibility gap, while the A–water system has a larger miscibility gap, but exhibits no azeotrope, and the A–C system exhibits neither an azeotrope nor a miscibility gap. Species A is the most volatile compound (normal boiling point of 40°C) and species C is the heaviest compound (normal boiling point of 144°C).

Next, the ternary system is considered. Fig. 3 shows the residue curves and binodal curve at 32.2°C. Note that the residue curves are computed assuming vapor–liquid equilibrium. The binodal curve is computed at 32.2°C to approximate the binodal curve at the higher temperatures at which vapor–liquid–liquid equilibrium exists. There are four singular points, three at the vertices and one at the water–C azeotrope. Because the minimum-boiling azeotrope is at a higher temperature than the boiling point of species A, a distillation boundary connects vertex A with the C–water azeotrope. Consequently, the operating line, or residue curve, for a simple distillation process cannot cross this distillation boundary.

2.2. Distillation tower

In this section, the proprietary distillation tower is described. Results of steady-state simulations are compared with experimental temperature profiles from an industrial tower in the next section.

The tower consists of 34 trays with a liquid feed to tray 16 and a sidedraw from tray 12. It is modeled, assuming an overall efficiency of 70%, with 23 theoretical trays, a liquid feed to tray 12, as shown in Table 1,

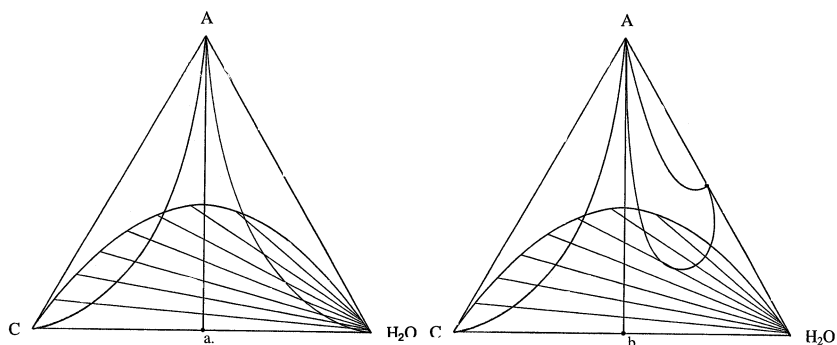


Fig. 1. Residue-curve map for the A–H₂O–C system.

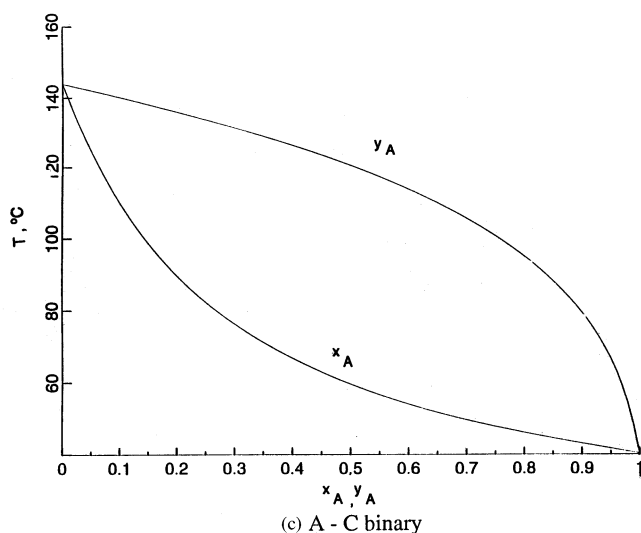
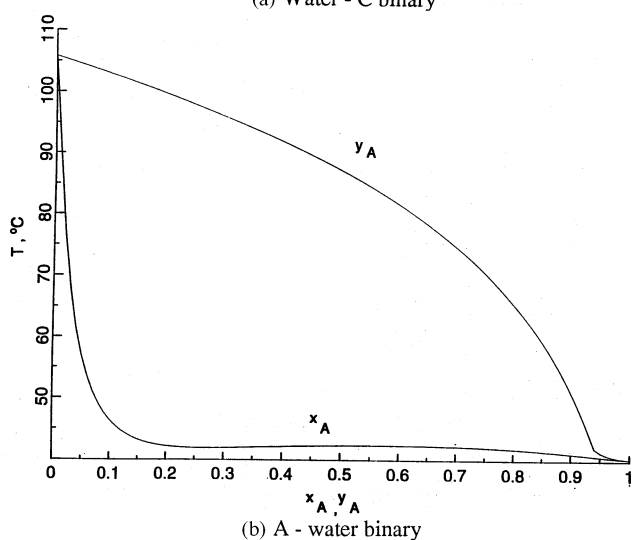
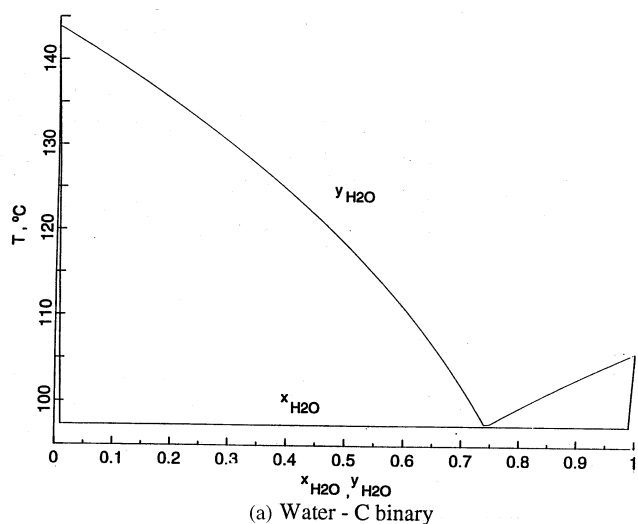


Fig. 2. Bubble- and dew-point temperatures for binary pairs at near-atmospheric pressure. (a) Water-C binary. (b) A-water binary. (c) A-C binary.

and a sidedraw from tray 9. Depending on the operating conditions, some of the trays contain both aqueous and organic phases. The sidedraw removes some of the aqueous phase flowing from tray 9, while the organic phase flows to the tray below. This is accomplished using a built-in 'donut' decanter tray that collects the liquid flowing from the tray above and permits phase separation, as illustrated in Fig. 4. The cavity in the center of the tray carries both the vapor, rising to the tray above, and the overflowing organic phase. An interfacial level controller maintains the position of the interface between the aqueous and organic phases and prevents the organic phase from escaping in the sidedraw and the aqueous phase from overflowing to the tray below. It does not prevent entrainment and does not insure perfect phase separation.

2.3. Steady-state simulation

The RADFRACTM subroutine in ASPEN PLUS was used to simulate the distillation column. RADFRAC can associate a decanter with any tray in the tower. Phase stability is checked on every stage to determine whether or not a second liquid phase exists. The decanter tray is modeled by specifying the fraction of each liquid phase to be returned to the tower, L1 and L2, for the organic and aqueous phases, respectively. When L1 is specified as unity and L2 is zero, the decanter is assumed to be perfectly efficient with all of the organic phase returned to the tower, and all of the aqueous phase removed as a sidedraw. An imperfect decanter is modeled by specifying L1 less than unity and/or L2 greater than zero.

The simulation was tuned to fit an experimental temperature profile by varying L2, while keeping L1 at unity. As shown in Fig. 5, when L2 is zero, the temperature profile of the model does not match the experimental data in the rectifying section. For $L2 < 0.47$, significant differences between the experimental and theoretical profiles exist in the rectifying section, whereas for $L2 > 0.49$, the differences are primarily in the stripping section. Only at $L2 = 0.48 (\pm 0.005)$ is there good agreement everywhere, as illustrated in Fig. 6.

In normal operation, none of the aqueous phase is recycled. However, since good agreement is obtained when the recycle fraction L2 is specified at 0.48, the water flow rates in the tower are higher than expected. One possible explanation is that the level controller of the decanter tray may not be functioning properly, and consequently, the entire aqueous phase may not be removed, resulting in the buildup and overflow of the aqueous phase. Another explanation would be the failure of the two liquid phases to separate completely due to an insufficient tray volume. This would result in the entrainment of water in the organic phase. By recycling a fraction of the aqueous phase below the decanter tray, these effects appear to be simulated adequately.

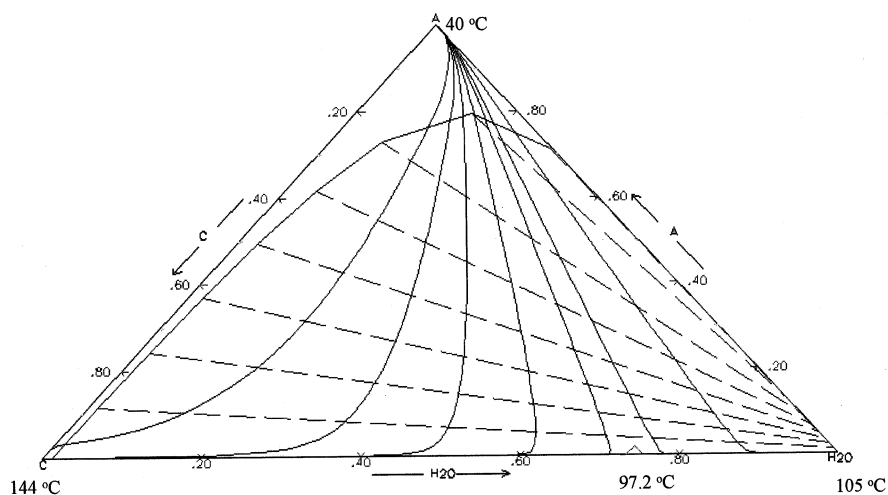


Fig. 3. Residue-curve map for the A–H₂O system.

To further clarify the heterogeneous operation in the tower, the average and individual liquid phase compositions are plotted on a triangular diagram in Fig. 7. Note the steep tie-lines that connect the phases in liquid–liquid equilibrium and the distillation boundary (not shown exactly), discussed above. Normally, distillation boundaries cannot be crossed by the operating lines in a distillation tower, except when the boundaries exhibit sizable curvature. However, due to liquid-phase splitting the aqueous phase on tray 9 can be removed, enabling the operating line to cross the distillation boundary. In this way, the partial miscibility of the system is used to advantage. A related observation is that water, the intermediate boiler, concentrates in the center of the tower. It is removed effectively in the sidedraw thanks to the partial miscibility of the system.

Fig. 7 also shows that, in the rectifying section, the temperature profile has two plateaus. The first encompasses trays 5–9, where the overall (three phase) compositions are close to the distillation boundary. The water–C ratio approaches that at the water–C azeotrope and, since the mole fraction of species A is small, the temperature remains nearly constant. On trays 2–4, as the two liquid phases coalesce, most of the separation occurs and the temperature drops as species A is dehydrated. On trays 1 and 2, the second liquid phase is no longer present, and the temperature profile reaches a second plateau as species A is purified.

Due to the removal of water in the sidedraw, the second liquid phase disappears between trays 10 and 11. Note that the binodal curve in Fig. 7 is computed at 32.2°C, which is far below the temperatures on trays 10 and 11; hence, it does not lie between points 10 and 11 in Fig. 7. Between trays 10 and 15, the temperature increases rapidly as species A is stripped from species C. Below tray 15, a third temperature plateau corresponds to small concentration changes as highly-pure C is produced.

Table 1
Feed conditions

		Weight fraction
$T = 126.7^\circ\text{C}$	A	0.1043
$P = \text{near atmospheric}$	Water	0.0153
Saturated liquid	C	0.8804
		1.0000

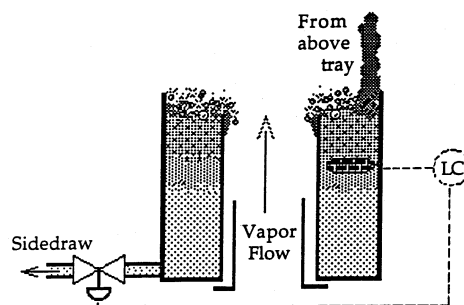


Fig. 4. Decanter tray with sidedraw.

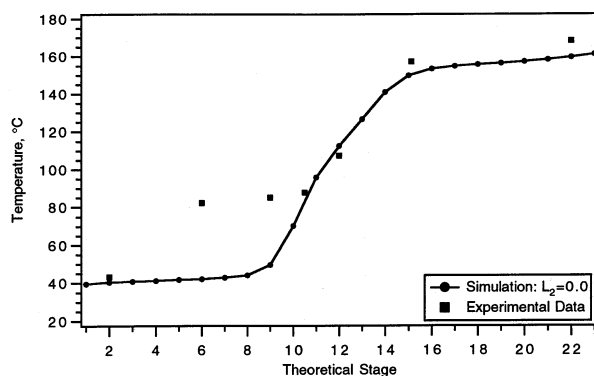


Fig. 5. Temperature profiles. Simulation results for $L_2 = 0$.

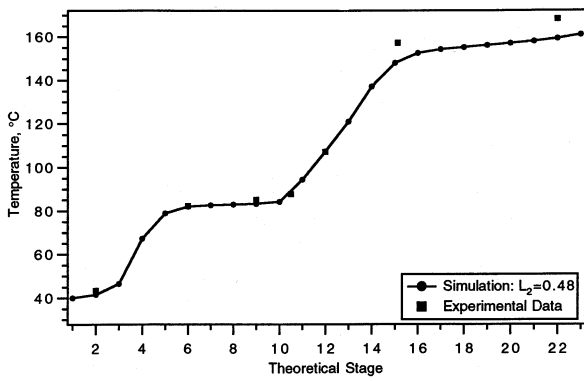


Fig. 6. Temperature profiles. Simulation results for $L_2 = 0.48$.

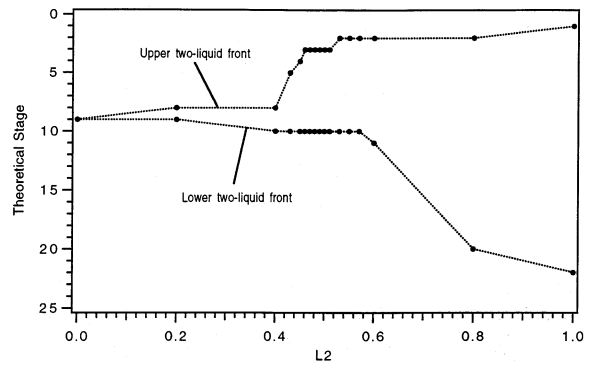


Fig. 8. Trays having two liquid phases (within dashed envelopes) as L_2 varies.

2.4. Sensitivity analysis

As mentioned above, the column responds very sensitively to the recycle fraction of the aqueous sidedraw. This can be seen in the responses of the two-liquid phase region. First, Fig. 8 shows that the two-liquid phase region expands as the flow rates of water in the column increase. At zero recycle, two liquid phases appear in the decanter tray only. At the other extreme, when the aqueous phase is completely recycled, two liquid phases appear on every tray except the reboiler. Note that the upper interface, between trays having two and one liquid phase(s), is especially sensitive when the recycle fraction varies between 0.4 and 0.5. Also, when increasing the fraction of the aqueous phase recycled, the second liquid phase does not advance into the stripping section until all of the stages in the rectifying section contain two liquid phases.

Similarly, the temperature and composition profiles are extremely sensitive to the fraction of the aqueous phase recycled. When none of the aqueous phase is recycled, the bulk of the separation occurs between

trays 8 and 15, where the temperature gradient is constant as shown in Fig. 5. First, species A is separated from water at the bottom of the rectifying section, and then from species C at the top of the stripping section, leaving nearly constant temperatures and compositions between trays 1–7 and 16–23. These profiles are not affected significantly as the recycle fraction is increased to 0.4. Although the composition of water increases substantially, only one additional tray has two liquid phases, beyond the decanter tray. However, as the recycle fraction increases toward 0.45, the separation between species A and water is shifted up the tower. A region, dilute in species A, involving water and C phases, spreads into the rectifying section, creating temperature and composition plateaus above the decanter tray, as shown in Fig. 9. From 0.45 to 0.48, the separation of species A from species C begins to move down in the stripping section. This movement is drastic from 0.48 to 0.49, as shown in Fig. 10. It is accompanied by a sharp increase in the concentration of species A in the stripping section, as shown in Fig. 11. Further increases of the recycle fraction further

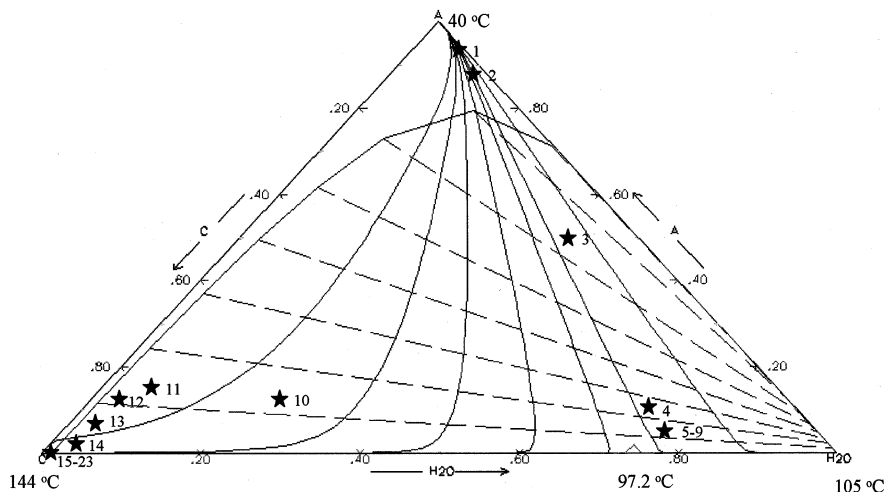


Fig. 7. Operating points for the simulated tower at $L_2 = 0.48$; average liquid mole fractions. * are calculated by RADFRAC.

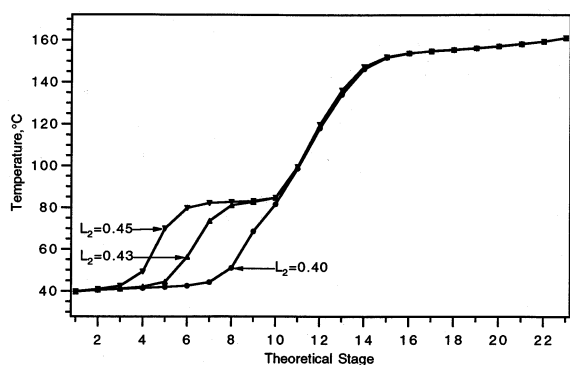


Fig. 9. Temperature profiles. Simulation results for $L_2 = 0.4, 0.43$ and 0.45 .

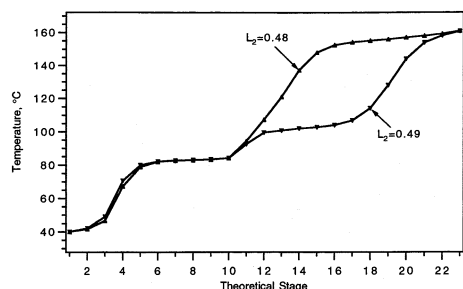


Fig. 10. Temperature profiles. Simulation results for $L_2 = 0.48$ and 0.49 .

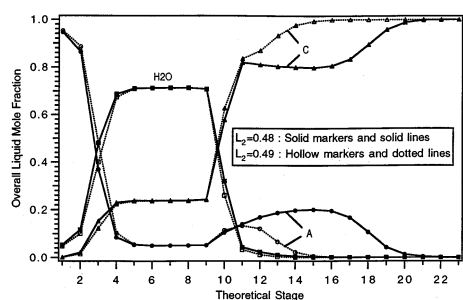


Fig. 11. Overall mole fractions in the liquid phases. Simulation results for $L_2 = 0.48$ and 0.49 .

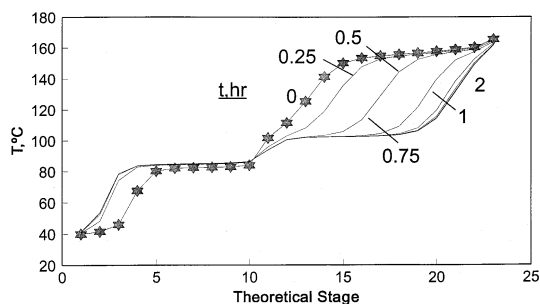


Fig. 12. Temperature response to a step increase in the weight fraction of water in the feed (0.0153 to 0.0191). $L_2 = 0.48$ at the initial steady state.

concentrate species A and spread the temperature composition plateaus.

On the basis of the steady-state simulations, it seems clear that the embedded two-liquid phase region is desirable. Sufficient water is needed to allow the embedded region to contract, without coalescing, when the water concentration in the feed decreases. However, as the region expands (especially for $L_2 > 0.48$) the losses of species A increase in the sidraw and the bottoms product. To select a desirable operating strategy with an embedded two-liquid phase region, dynamic simulations, with and without controllers, are helpful, as described next.

2.5. Process dynamics

Dynamic simulations are carried out with the SPEEDUP system. The trays in the rectifying section have a residence time of clear liquid between 23 and 29 s, whereas the residence time is much smaller in the stripping section, between approximately 2.5 and 3.5 s. The decanter tray, reflux accumulator, and reboiler have residence times of approximately one-third hour, between 2.7 and 5.4 min, and approximately 9.6 min, respectively.

The trays are modelled with the Francis Weir Formula. The MESH (Material balance, Equilibrium, Summation of mole fraction, and Heat balance) equations include terms that represent the enthalpy and flow rates of the species in a second liquid (aqueous) phase. Note that when the aqueous phase does not exist, the flow rate variables are zero. Furthermore, during each time step, the stability of the phase distribution on each tray is checked using tangent-plane-distance analysis (Michelsen, 1982). When the distribution is unstable, a liquid phase is added or deleted as necessary. For this tower, this stability analysis is critical in the dynamic simulations to permit the two interfaces between trays having two and one liquid phase(s) to be tracked properly in response to typical disturbances. This is established in a similar tower, involving the dehydration of *sec*-butanol, by Widagdo, Seider and Sebastian (1992). In the results that follow, this movement seems reasonable, although confirmation with experimental data has not been accomplished.

The tower simulations begin at steady states with the recycle fraction of the aqueous sidraw (L_2) at 0.48 and 0.49. At $L_2 = 0.48$, two liquid phases exist on the decanter tray but not further down into the stripping section. At $L_2 = 0.49$, the aqueous phase moves far down into the stripping section. First, open-loop simulation results are presented to show the movement of the interface below the decanter tray, beginning with $L_2 = 0.48$, after an increase in the weight fraction of water in the feed from 0.0153 to 0.0191 (holding the weight fraction of species A fixed). Fig. 12 shows the movement of the temperature front, which corresponds

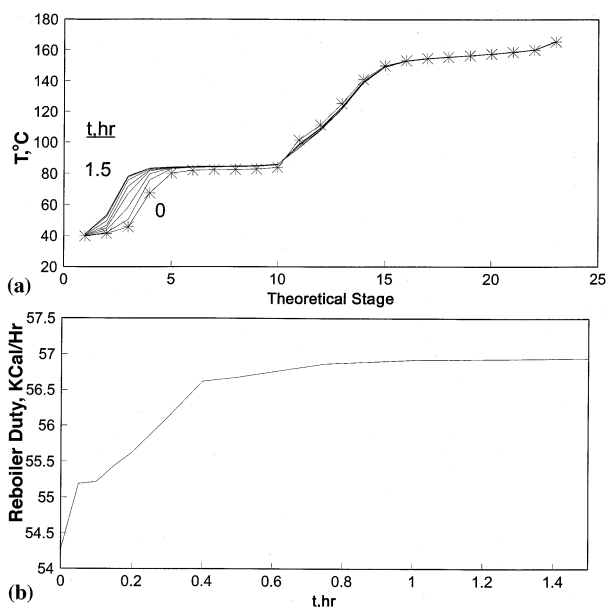


Fig. 13. Responses to a step increase in the weight fraction of water in the feed (0.0153 to 0.0191) with PI control. $L2 = 0.48$. (a) Temperature. (b) Reboiler heat duty.

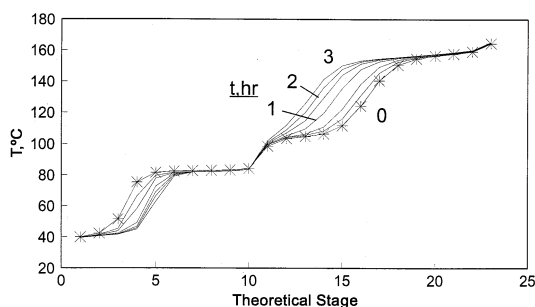


Fig. 14. Temperature response to a step decrease in the weight fraction of water in the feed (0.0153 to 0.0141). $L2 = 0.49$ at the initial steady state.

to the interface between stages having two and one liquid phase(s), to a new steady state in about 2 h. This figure also shows that the interface moves up in the rectifying section. Note that the temperature profile at $L2 = 0.49$ in Fig. 10, computed using ASPEN PLUS, is not identical to that in Fig. 12, computed using SPEEDUP. This is because the initial conditions for the dynamic simulation are not exactly at the steady state corresponding to $L2 = 0.49$.

These studies were repeated with a PI controller which measures the temperature on tray 15 and attempts to maintain the set point (150°C at the $L2 = 0.48$ steady state) by adjusting the reboiler heat duty. The responses, with a controller gain and reset time equal to 2 and 54.27, respectively, are shown in Fig. 13. Observe that the controller maintains the temperatures and compositions below the decanter tray with rather small changes in the boilup rate. However, the move-

ments in the rectifying section are substantial as the composition and temperature fronts move closer to the condenser. To avoid a break-through, a temperature measurement in the rectifying section, coupled with another manipulated variable, such as the reflux rate, may be desirable. Alternatively, it may be possible to prevent the movement in the rectifying section with a model-predictive controller (MPC) that incorporates the SPEEDUP model within an optimization algorithm.

Figs. 14 and 15 repeat these simulations, beginning with the steady state at $L2 = 0.49$, and a decrease in the weight fraction of water in the feed from 0.0153 to 0.0141. Fig. 14 shows that, without the controller, the interfaces move upward in the stripping section and downward in the rectifying section. With the controller, as shown in Fig. 15, the movement in the stripping section is negligible. In the rectifying section, however, the movement is substantial, but away from the condenser. Note that, in this case, the temperature set point on tray 15 is 111.74°C (at the $L2 = 0.49$ steady state) and the time to reach the new steady state is approximately 4 h.

These results highlight some of the considerations in controlling such a sensitive tower that contains an imbedded two-liquid phase region. They are presented to suggest important issues in developing model-based controllers.

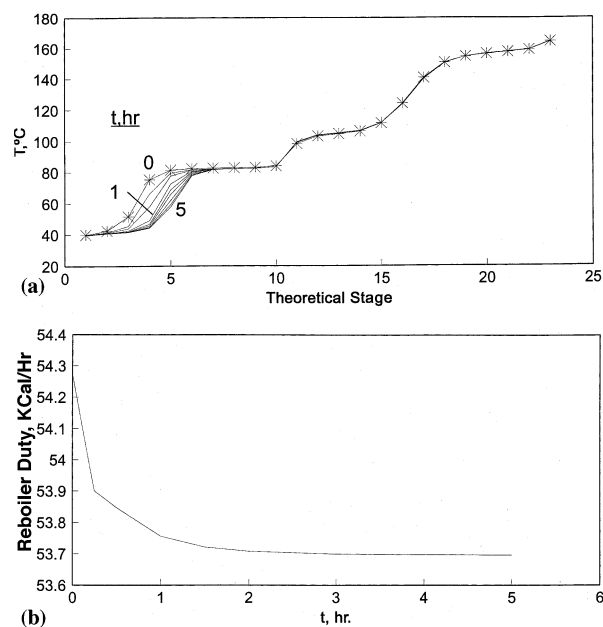


Fig. 15. Responses to a step decrease in the weight fraction of water in the feed (0.0153–0.0141) with PI control. $L2 = 0.49$. (a) Temperature. (b) Reboiler heat duty.

Table 2
Feed stream for multiplicity studies

		Mole fraction
$T = 84.4^\circ\text{C}$	A	0.173
$P = 1.2 \text{ bar}$	Water	0.084
$F = 10.566 \text{ kmol/h}$	B	0.477
	C	0.002
	D	0.025
	E	0.239
		1.000

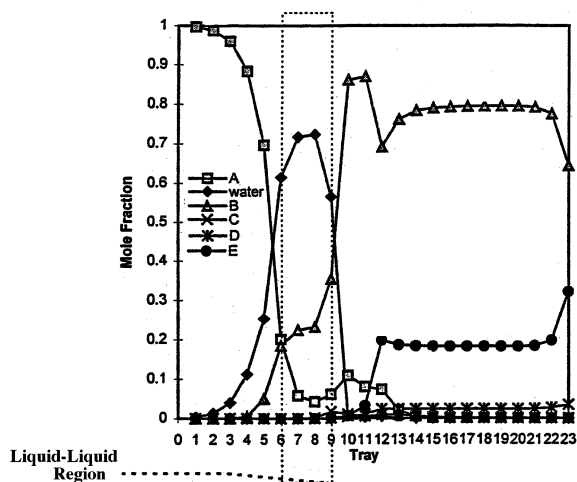


Fig. 16. Profiles of average mole fractions in the liquid phases — Solution I.

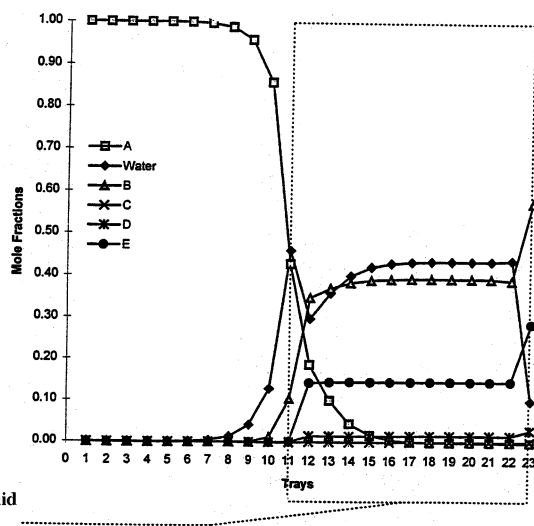


Fig. 17. Profiles of average mole fractions in the liquid phases — Solution II.

3. Multiple steady states

Having concentrated on the analysis of the tower with three species, A, water, and C, in this section, the analysis is extended to include organic species B, D, and E. Note that, in the ternary mixture, species C best represents the combination of species B, C, D, and E,

in the multicomponent mixture. Two regions of multiple steady states are observed, one involving the partial miscibility of the C–water pair, as above, and the other involving the partial miscibility of the B–C pair.

For the calculations that follow, the MESH equations are solved using the RADFRAC model in ASPEN PLUS, Version 9.3-2, with vapor–liquid–liquid equilibrium modeled using UNIFAC. Most of the interaction parameters are in the ASPEN PLUS database, with the exception of those for the groups in species D and E which are estimated.

For the feed stream in Table 2, the first region of multiple steady states is computed with the distillate flow rate specified at 1.825 kmol/h, equal to the flow rate of species A in the feed, and the reboil ratio specified at unity. Two steady-state solutions are computed. The first corresponds to the desired regime, with two liquid phases on trays 6–9, a reflux ratio of 2.66, and a sidraw flow rate of 0.914 kmol/h. The second, anomalous, solution has two liquid phases on trays 11–23, a reflux ratio of 5.79, and zero sidraw flow rate. The corresponding profiles of liquid-phase mole fractions appear in Figs. 16 and 17. In the first solution, species A is concentrated (> 90 mol%) on trays 1–3, while in the second solution, species A is concentrated on trays 1–9. Similarly, in the first solution, the mole fraction of water peaks on tray 8, and in the second solution, it peaks on tray 11.

A closer examination of the second solution shows that the bottoms flow rate is increased. For specified distillate flow rate and reboil ratio, the reflux ratio and vapor boilup are increased as explained below, assuming constant molar overflow. Beginning with the reflux splitter, the overall mass balance is:

$$V = D + L \quad (1)$$

and the reflux ratio is defined:

$$L = RD \quad (2)$$

Then, at the feed tray, the overall mass balance is:

$$V = V' + qF \quad (3)$$

and the reboil ratio is defined:

$$V' = R'B \quad (4)$$

Here, F is the feed flow rate, D and B are the distillate and bottoms flow rates, V and V' are internal vapor flow rates in the rectifying and stripping sections, L is the liquid flow rate in the rectifying section, q is the feed quality, and R and R' are the reflux and reboil ratios.

With $q = 0$, Eqs. (1)–(3) combine to:

$$R = R'B/D - 1 \quad (5)$$

In the first operating regime, the bottoms flow rate is approximately equal to H , the flow rate of heavy organics (species B–E) in the column feed. Substituting in Eq. (5):

$$R_I = R'H/D - 1 \quad (6)$$

In the second regime, since the sidedraw flow rate is zero, and all of the water leaves in the bottoms product, the reflux ratio is:

$$R_{II} = R'(H + W)/D - 1 \quad (7)$$

where W is the flow rate of water in the feed stream.

With $R_{II} > R_I$, the purity of the distillate product increases and the top trays become more concentrated in species A. Hence, the water profile is displaced down the column. If the reflux ratio is sufficiently high, the A–water front is displaced below the decanter tray, and consequently, only one liquid phase remains on the decanter tray.

3.1. Transitions between regimes

When the column is operating in the normal regime, there are two disturbances that trigger a transition from one operating regime to another, as described next.

3.1.1. Increased heavy organics feed rate

For a fixed reboil ratio, additional heavy organics leave in the bottoms product and the boilup flow rate increases proportionately. When the distillate flow rate is fixed also, the reflux increases, as does the reflux

ratio. The higher reflux ratio increases the purity of the distillate, with the mole fraction of species A increasing throughout the rectifying section. As species A moves down the column, trays having two liquid phases are displaced downward. The aqueous phase disappears from the decanter tray and water appears in the bottoms product, further increasing the boilup flow rate and reinforcing the transition into the anomalous regime.

3.1.2. Increased light organic feed rate

The increased feed rate causes species A to concentrate in the rectifying section, displacing water and causing the liquid–liquid region to move down the column below the decanter tray. This is accompanied by a decrease in the flow rate of the aqueous sidedraw. As the sidedraw flow rate drops, the bottoms flow rate increases, resulting in a higher boilup rate, a larger reflux ratio, purer distillate product, and the further accumulation of species A in the rectifying section.

This transition is illustrated in Fig. 18. Here, the sidedraw flow rate is a function of the ratio of the distillate flow rate to the feed rate of species A. Notice that two solutions are shown at ratios close to unity. When the ratio is less than one, the column operates without a sidedraw; when greater than one, an aqueous sidedraw exists. As the ratio decreases, due to increasing feed rate of species A, the column moves from one regime to the other. Note that, thus far, a third intermediate solution has not been computed, which unlike the two solutions shown, must be unstable.

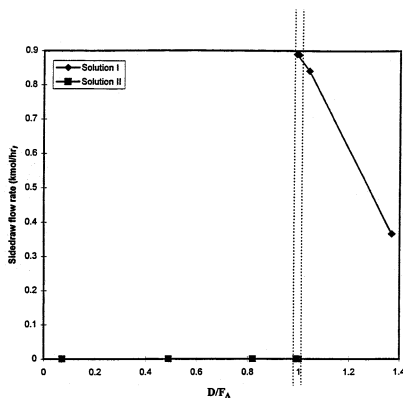


Fig. 18. Sidraw flow rate as a function of the distillate/feed A ratio.

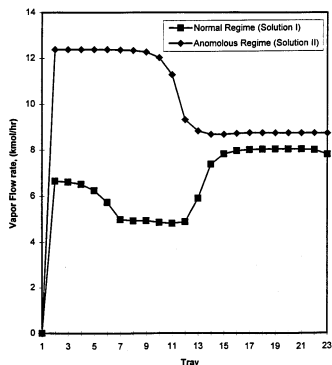


Fig. 19. Profiles of internal vapor flow rates.

3.2. Transitions and malfunctions

Transitions toward the anomalous regime may be responsible for the flooding malfunctions often reported in these columns. At low pressures, the gas velocity, v , is related to the internal vapor flow rate, V , by:

$$v = RTV/PA \quad (8)$$

where R is the universal gas constant, T is the absolute temperature, P is the pressure, and A is the cross-sectional area. The factor R/PA is the same in both regimes, and, since species A concentrates near the top of the column in both regimes, the temperatures at the top of the column are the same as well. Hence, the gas velocity is proportional to the internal vapor flow rate.

Fig. 19 shows that near the top of the column, the internal vapor flow rate, V , in the anomalous regime is approximately twice that in the normal regime. Consequently, the gas velocity is nearly doubled during a transition from the normal to the anomalous regime. Since most columns are not designed to handle such a large increase in the gas velocity, flooding is anticipated before the anomalous regime is reached.

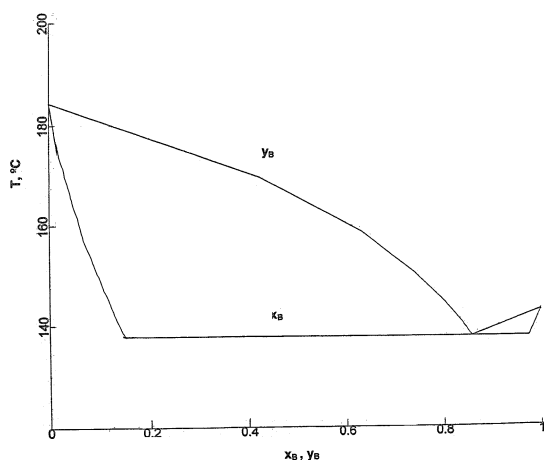


Fig. 20. Bubble- and dew-point temperatures of B–C mixture at 1.22 bar.

4. Organic sidedraw

The second region of multiple steady states is computed at constant reflux and bottoms flow rates. In this case, one of the steady-state solutions exhibits two organic phases because species B and C exhibit a wide miscibility gap with a minimum-boiling heterogeneous azeotrope at 85 mol% B and 138°C, as shown in Fig. 20. At constant reflux flow rate and low bottoms flow rate, species B appears in the distillate and the decanter tray separates a B-rich phase from a C-rich phase, in the absence of a water phase.

Fig. 21 shows the sidedraw flow rate as a function of the bottoms flow rate when the reflux flow rate, L , is 3.5 kmol/h. When the bottoms flow rate is less than 7.3 kmol/h, only one solution is computed, with one liquid phase on the decanter tray and zero sidedraw flow rate. In a narrow region surrounding 7.3 kmol/h, two solutions are computed, the first having one liquid phase on the decanter tray and zero sidedraw flow rate, and the second having two liquid phases on the decanter tray and a small sidedraw flow rate (0.015 kmol/h). For

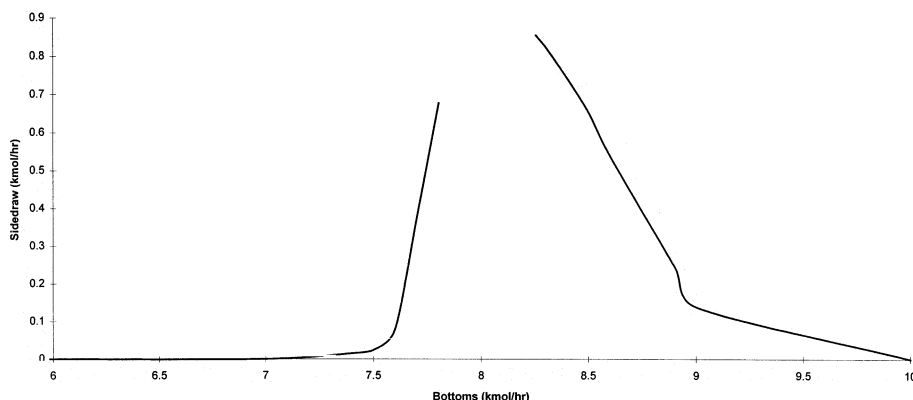


Fig. 21. Sidedraw flow as a function of bottoms flow rate.

bottoms flow rates between 7.3–7.8 and 8.25–10 kmol/h, one solution is computed with a sidedraw stream, with the sidedraw disappearing at 10 kmol/h. Note that the RADFRAC subroutine could not compute solutions for bottoms flow rates between 7.8 and 8.25 kmol/h. While this void is disappointing and not yet explained, it seems clear that this operating regime deserves further study, possibly using global convergence techniques such as differential arc-length homotopy-continuation as well as experimental verification.

In the first regime, when the bottoms flow rate is less than 7.3 kmol/h, species A, water, and species B and C, leave as distillate with species D and E concentrating in the bottoms product. There is a plateau extending down into the rectifying section in which the liquid phase is comprised almost entirely of species A and B. Below this plateau, the concentrations of species A and B drop as species D and E become more concentrated. The concentrations of water and species C are less than 1 mol% everywhere except on the top tray, where two liquid phases exist, with one liquid phase on the other trays.

When the sidedraw appears, the top three trays contain a quaternary mixture of water, and species A, B, and C. From trays 4–9, the liquid contains a ternary mixture of species A, B, and C. As shown in Fig. 22, these mixtures contain approximately 5 mol% A, 84–90 mol% B, and 5–10 mol% C, which separate into B-rich and C-rich phases having densities of 0.8 and 1.4 g/ml, respectively. Note that the distillate stream contains 28 mol% water, 58 mol% A, 14 mol% B, and a small concentration of species C.

As the bottoms flow rate increases, the amount of water in the sidedraw increases. When the bottoms reaches 7.8 kmol/h, the side stream is 96 mol% water and 3.6 mol% C. At 8.25 kmol/h, the sidedraw stream contains 99.5 mol% water and 0.5 mol% A, and the concentration profiles within the column are changed significantly, with no appreciable concentration of species C remaining in the column.

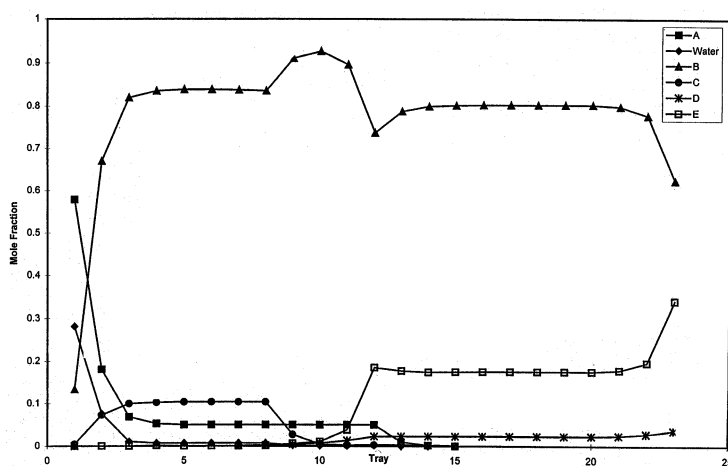


Fig. 22. Composition profile for $B = 7.3$ kmol/h.

Potentially, there are two reasons no solution is computed for bottoms flow rates from 7.8–8.25 kmol/h. Since the total feed rate of species B, C, D, and E is 7.8 kmol/h, as the bottoms flow rate increases above 7.8 kmol/h, water moves from the sidraw to the bottoms product, and the embedded liquid–liquid region moves from trays 2–10 to trays 7–22. This abrupt transition may be accompanied by steep gradients, with associated numerical problems. Alternatively, an unexplained physical mechanism might be needed to show that solutions are not feasible in this region.

5. Conclusions

In distillation columns with internal decanters, the steady-state regimes and dynamic transitions show unusually sensitive behavior patterns and tendencies to move from one steady state to another. This has been demonstrated herein for a proprietary tower involving a mixture of oxygenated hydrocarbons and water. On the basis of simulation studies, with limited experimental results, it is concluded that these towers, for the separation of multiple azeotropes with partial miscibility have complex solution spaces, and need to be characterized more completely.

More specifically, for the simulations and experimental data reported herein, it is concluded that:

1. When operating in the normal regime, the overall effect of changing the aqueous recycle fraction of the sidraw is to change the positions of the two separations, species A from water, and species A from species C. When the recycle fraction is zero, both separations occur near the center of the tower, with temperature and composition plateaus located at the top and bottom of the tower. At the other limit, when the recycle fraction is unity, the temperature and composition plateaus are located in the

middle of the tower and the separations occur at the extremes of the tower.

2. At an aqueous recycle fraction of 0.48, the computed temperature profile closely approximates the temperature measurements. Under these conditions, the aqueous phase extends from the decanter tray upward into the rectifying section, but not below the decanter tray. Whereas at an aqueous recycle fraction of 0.49, the aqueous phase extends downward below the decanter tray. This sensitivity suggests difficult operating problems.
3. To reject typical disturbances, such as changes in the concentration of water in the feed stream, it is desirable to operate with two liquid phases in the rectifying section and below the decanter tray. For disturbances involving the amounts of the heavy or light organic species in the feed stream, care must be taken to avoid a shift toward a second steady state, without a sidraw and with larger flow rates of bottoms product and boilup, which could lead to flooding.
4. The dynamic simulations about the normal regime show that a single PI control loop can reject these disturbances nicely, but not perfectly. Additional measurements and manipulated variables, together with model-predictive control, show promise for even better operation in this sensitive regime.
5. At constant reflux and low flow rates of the bottoms product, the partial miscibility of species B and C can express itself in an anomalous steady state in which two organic liquid phases appear on the decanter tray, one of which is removed in the sidraw. This steady state is shown for the first time in this paper. Further studies are needed to examine the kinds of disturbances that can lead to this regime of operation, their dynamic responses and associated control issues.

6. Nomenclature

A	cross-sectional area (m^2)
D	distillate flow rate (kmol/s)
F	feed flow rate (kmol/s)
H	flow rate of heavy organic species (B–E) in the column feed (kmol/s)
L	reflux flow rate (kmol/s)
$L1$	fraction of organic phase in sidedraw sent to tray 10
$L2$	fraction of aqueous phase in sidedraw sent to tray 10
P	pressure (bar)
q	quality of feed
R	reflux ratio (L/D); Universal gas constant
R'	boilup ratio (V'/B)
t	time (s)
T	temperature (K)
v	gas velocity (m/s)
V	vapor flow rate from rectifying section (kmol/s)
V'	boilup rate (kmol/s)

W flow rate of water in feed stream (kmol/s)

Subscripts

A	species A
I	regime I
II	regime II

Acknowledgements

Partial support was provided by the National Science Foundation under Grants No. EEC 952 7441 and CTS-9904099 and is gratefully acknowledged.

References

- Michelsen, M. L. (1982). The isothermal flash problem I: stability. *Fluid Phase Equilibria*, 9, 21.
- Widagdo, S., Seider, W. D., & Sebastian, D. H. (1992). Dynamic analysis of heterogeneous azeotropic distillation. *American Institute of Chemical Engineering Journal*, 38, 1229.
- Widagdo, S., & Seider, W. D. (1996). Azeotropic distillation — a review. *American Institute of Chemical Engineering Journal*, 42(1), 96–130.